INTERNATIONAL JOURNAL OF ADAPTIVE CONTROL AND SIGNAL PROCESSING, VOL. 5, 107–120 (1991)

MODEL REFERENCE ADAPTIVE CONTROL FOR THE AZIMUTH-POINTING SYSTEM OF A BALLOON-BORNE STABILIZED PLATFORM

ALFREDO O. CHINGCUANCO,* PHILIP M. LUBIN AND PETER R. MEINHOLD†
Department of Physics, University of California, Santa Barbara, CA 93106, U.S.A.

AND

MASAYOSHI TOMIZUKA
Mechanical Engineering Department, University of California, Berkeley, CA 94720, U.S.A.

SUMMARY

A balloon-born stabilized platform has been developed for the remotely operated altitude-azimuth pointing of a millimetre wave telescope system. This paper presents a development and implementation of model reference adaptive control (MRAC) for the azimuth-pointing system of the stabilized platform. The primary goal of the controller is to achieve pointing RMS better than $0{\cdot}1^{\circ}$. Simulation results indicate that MRAC can achieve pointing RMS better than $0{\cdot}01^{\circ}$. Ground test results show pointing RMS better than 0.03°. Data from the first flight at the National Scientific Balloon Facility (NSBF), Palestine, TX show pointing RMS better than $0{\cdot}02^{\circ}$.

KEY WORDS Adaptive control Discrete time control Application

1. INTRODUCTION

A balloon-borne stabilized platform, as shown in Figure 1, was developed at the Physics Department of the University of California, Santa Barbara, CA and is used for sensitive measurements of anisotropy in the cosmic background radiation (CBR), a remnant of the Big Bang. The platform is suspended under a 100 000 m^3 zero-pressure helium-filled balloon, as shown in Figure 2. The balloon floats at an altitude of ~ 30 km.

Azimuth pointing of the platform is achieved by torquing directly into inertial space with the use of the reaction wheel system shown in Figure 3. The flywheel or reaction wheel is spun up by the torque motors, causing the gondola to react in the opposite direction. As the reaction wheel operates to keep the gondola pointed correctly, the flywheel will eventually be accelerated to a high angular velocity to the point that the back EMF produced prevents any more torquing capability. This condition is referred to as the flywheel reaching saturation.

* Graduate student, Mechanical Engineering Department, University of California, Berkeley, CA, U.S.A.
† Graduate student, Physics Department, University of California, Berkeley, CA, U.S.A.

This paper was recommended for publication by editor R. Bitmead

0890–6327/91/020107–14$07.00

Received 5 July 1989
Revised September 1990

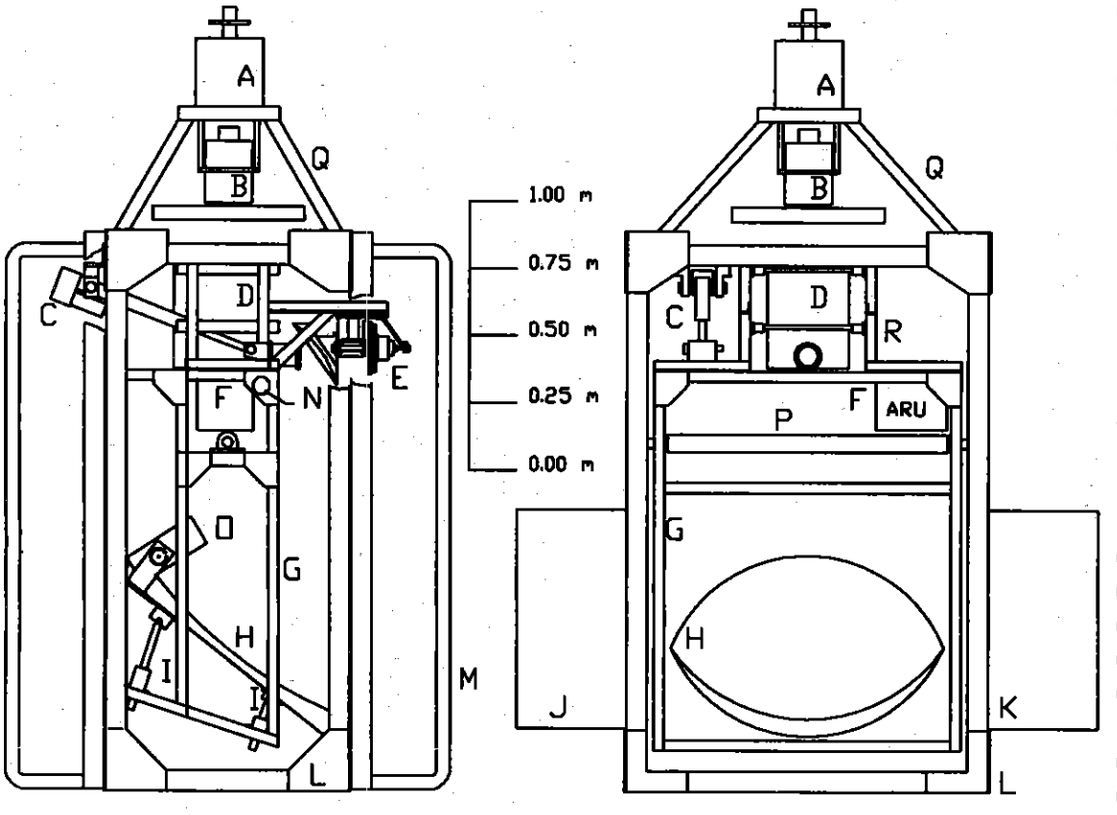

Figure 1. Gondola structural lay-out and main components

(A) RCUBE
(B) Reaction Wheel
(C) Linear Actuator
(D) Dewar
(E) Nutation System /Secondary Mirror
(F) ARU Gyroscope
(G) Secondary Frame
(H) Off Axis Parabolic Mirror
(I) Adjustable Mirror Mount
(J) Electronics/ Computer Box
(K) Telemetry/ Battery Box
(L) Main Frame
(M) Roll Bars
(N) Clinometer
(O) CCD Camera
(P) Main Elevation Shaft
(Q) Top Spider Frame
(R) Dewar Mount
* Magnetometer inside Box (J)

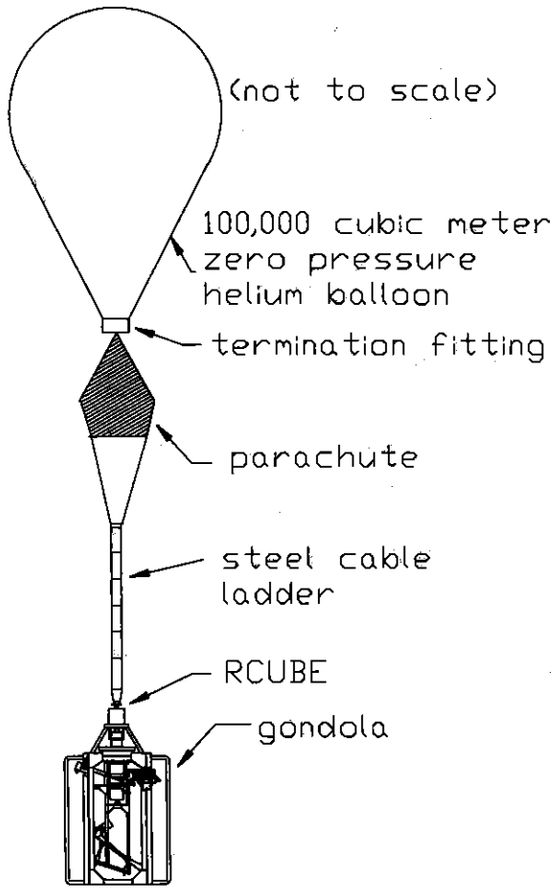

Figure 2. Balloon-borne stabilized platform

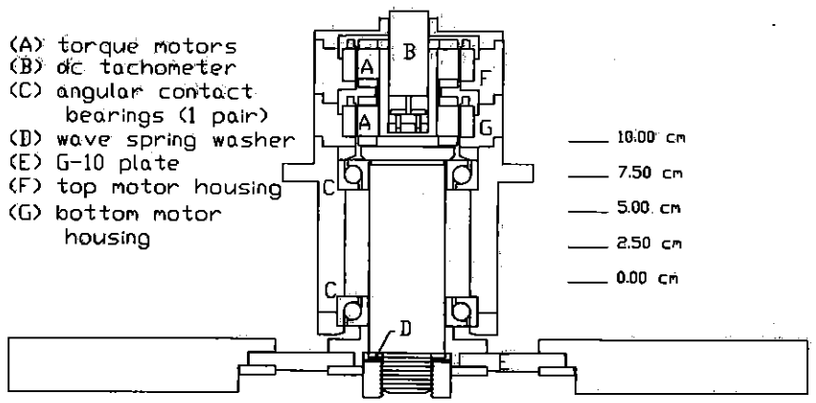

Figure 3. Reaction wheel system

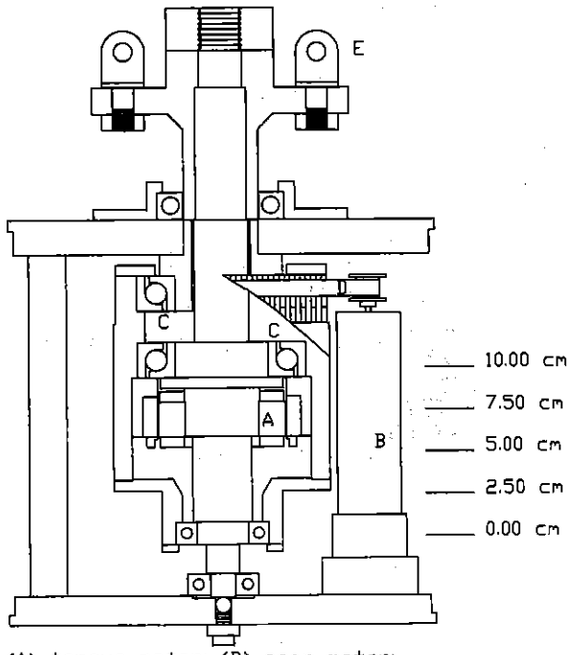

(A) torque motor; (B) gear motor;
(C) angular contact bearing (1 pair);
(D) timing belt; (E) three point
flight train connection
* Note: brushes and slip rings not shown

Figure 4. RCUBE, motor-driven double-bearing assembly

Desaturation can be done by despinning the flywheel, thus dumping angular momentum to the balloon. Intermittent desaturation, however, can result in the loss of valuable observation time during balloon flight.

In this experiment, continuous operation of the azimuth-pointing system is achieved with a desaturation device called the RCUBE, as shown in Figure 4. The RCUBE uses a set of two angular contact bearings. One bearing couples the gondola to the moving race, while the other couples the moving race to the balloon. The DC gear motor is used to drive the bearing housing in constant motion to avoid stiction during flight. The other motor, a torque motor, is used to torque the gondola against the balloon/flight train system. The RCUBE is used primarily to isolate or decouple the motion of the gondola from the balloon and to provide a desaturation mechanism for flywheel angular velocity.[1]

In Reference 2 a PID control with constant desaturation of the flywheel angular velocity was developed on the basis of a truncated system model. This controller was successfully implemented and was shown to be able to achieve the two goals of the azimuth controller, i.e. the primary goal of achieving steady state azimuth-pointing RMS of better than $0{\cdot}1^\circ$ and the secondary goal of maintaining the flywheel angular velocity below saturation to provide for continuous operation of the azimuth-pointing system. Actual flight data show pointing RMS better than $0{\cdot}02^\circ$ with the use of the PID controller.

In this paper a model reference adaptive control is developed for the azimuth-pointing system of a balloon-borne stabilized platform.

2. MOTIVATION FOR USING ADAPTIVE CONTROL

The nature of the experiment requires that the platform be operated at a float altitude of about ~30 km. Low ambient temperature of about -40° C, low atmospheric pressure and unaccounted changes in payload mass could affect the plant parameters used in designing deterministic-type controllers. Although the PID controller was able to achieve pointing RMS better than $0{\cdot}02^\circ$ during actual flight, it was imperative that a back-up controller be developed in case the PID control failed to work. Also, even if the parameter changes are known, control parameters will still have to be recomputed and time-consuming fine tuning of the gains may become necessary. Adaptive control is an attractive candidate as a back-up controller or for end users with little control background. Either the self-tuning approach or model reference adaptive control (MRAC) appears to be appropriate. In this paper MRAC is explored.

3. DEVELOPMENT OF MODEL REFERENCE ADAPTIVE CONTROL (MRAC)

The development of the equations for MRAC follows closely the presentation in Reference 3. First, two important assumptions crucial to the implementation of MRAC are made.

1. By keeping the bearing housing velocity large enough, i.e.

$$\omega_a - \omega_g > \omega_m/n_g \quad \omega_m < 0 \tag{1}$$

or

$$\omega_a - \omega_g < \omega_m/n_g \quad \text{for } \omega_m > 0 \tag{2}$$

where ω_a is the angular velocity of the RCUBE shaft, ω_g is the angular velocity of the gondola, ω_m is the angular velocity of the gear motor and n_g is the gear ratio from the bearing housing to the gear motor drive pinion, only 'unidirectional' Coulomb friction disturbance is experienced by the gondola.[2] This mode of operation is achieved by sending a constant voltage g_{volt} to the gear motor drive of the RCUBE. The preceding assumption allows for the adaptation of a constant or slowly varying DC disturbance.

2. At steady state operation the RCUBE control is implemented with

$$u_2 = g_{rbase} + k_v(\omega_f - \omega_{fref}) \tag{3}$$

where u_2 *is the D/*A command to the RCUBE torque motor, g_{rbase} is an offset voltage to the RCUBE torque motor, ω_f is the flywheel angular velocity, ω_{fref} is the reference flywheel angular velocity and k_v is the desaturation control gain. The desaturation control[2] $k_v(\omega_f - \omega_{fref})$ works to keep the flywheel operating near some steady state angular velocity below the saturation level and to minimize the effect of Coulomb friction torque, which is treated as a constant disturbance. Since the main cause of the saturation of the flywheel angular velocity is external disturbance, the desaturation control effectively uses the flywheel velocity information to generate pseudo-disturbance in order to maintain the flywheel angular velocity near some steady state value.

Assuming the desaturation control is working during steady state operation, it becomes possible to treat the azimuth-pointing system as simpler single-input/single-output (SISO) system with constant disturbance.

With these two assumptions the discrete time system model is written as

$$A(z^{-1})y(k) = z^{-d}B(z^{-1})u(k) + dc \tag{4}$$

where z^{-1} is the backward shift operator, $y(k)$ is the azimuth angle position at time k, $u(k)$ is the flywheel control u_1 at time k, dc is a constant disturbance, $A(z^{-1}) = 1 + a_1z^{-1} + a_2z^{-2} + \cdots + a_{n_A}a^{-n_A}$, n_A is the order of polynomial $A(z^{-1})$, $B(z^{-1}) = b_0 + b_1z^{-1} + b_2z^{-2} + \cdots + b_{n_B}z^{-n_B}$, n_B is the order of the polynomial $B(z^{-1})$ and d is the plant time delay.

The control objectives are as follows.

1. In tracking it is desired that the azimuth angle satisfies the equation

$$C_1(z^{-1})y(k) = z^{-d}D(z^{-1})u_m(k) \tag{5}$$

   where $C_1(z^{-1})$ is asymptotically stable and $u_m(k)$ is a bounded reference.
2. In regulation, with $u_m(k) = 0$, it is desired that the initial non-zero condition is eliminated while satisfying the equation

$$C_2(z^{-1})y(k+d) = 0 \tag{6}$$

   where $C_2(z^{-1}) = 1 + c_{21}z^{-1} + c_{22}z^{-2} + \cdots + c_{2n_{C2}}z^{-n_{C2}}$ is an asymptotically stable polynomial and n_{C2} is the order of polynomial $C_2(z^{-1})$.

A reference model used in the model reference adaptive control is

$$C_1(z^{-1})y_m(k) = z^{-d}D(z^{-1})u_m(k) \tag{7}$$

where $y_m(k)$ is the reference tracking azimuth angle. The control objectives are achieved by letting the error between $y_m(k)$ and the actual azimuth $y(k)$ vanish while satisfying

$$C_2(z^{-1})e^*(k+d) = 0 \tag{8}$$

$$e^*(k+d) = y(k+d) - y_m(k+d) \tag{9}$$

Using the Bezout identity

$$C_2(z^{-1}) = A(z^{-1})S(z^{-1}) + z^{-d}R(z^{-1}) \tag{10}$$

where $S(z^{-1}) = 1 + s_1z^{-1} + s_2z^{-2} + \cdots + s_{n_S}z^{-n_S}$, $R(z^{-1}) = r_0 + r_1z^{-1} + r_2z^{-2} + \cdots + r_{n_R}z^{-n_R}$, n_S $(= d-1)$ is the order of polynomials $S(z^{-1})$ and n_R $(= \max(n_A - 1, n_{C2} - d))$ is the order of polynomial $R(z^{-1})$, and substituting equation (9) in equation (8), we obtain

$$\begin{aligned} C_2(z^{-1})e^*(k+d) &= B(z^{-1})S(z^{-1})u(k) + R(z^{-1})y(k) + S(z^{-1})dc - C_2(z^{-1})y_m(k+d) \\ &= \mathbf{p}^T\boldsymbol{\phi}(k) - C_2(z^{-1})y_m(k+d) \end{aligned} \tag{11}$$

where

$$\mathbf{p}^T = [b_0, b_0s_1 + b_0, b_0s_2 + b_1s_1 + b_2, \ldots, b_{n_B}s_{n_S}, r_0, \ldots, r_{n_R}, dc^*]$$

$$\boldsymbol{\phi}^T(k) = [u(k), u(k-1), \ldots, u(k-d-n_B+1), y(k), \ldots, y(k-n_R), 1]$$

$$dc^* = S(z^{-1})dc \quad \text{(rescaled disturbance)}$$

Note that $dc^* = S(1)dc = \text{constant}$, except for the first $d-1$ steps.

The control $u(k)$ from equations (8) and (11) can be computed as

$$u(k) = (1/b_0)(C_2(z^{-1})y_m(k+d) - R(z^{-1})y(k) - Bs(z^{-1})u(k-1) - dc^*) \tag{12}$$

where $Bs(z^{-1}) = B(z^{-1})S(z^{-1}) - b_0$ and $Bs(z^{-1})$ is of order $n_{Bs} = n_B + d - 1$. The corresponding deterministic control block (linear-model-following control) is shown in Figure 5.

When the plant parameters are not known, the control objective becomes

$$\lim_{k\to\infty} C_2(z^{-1})(y(k) - y_m(k)) = 0 \tag{13}$$

and the control law becomes

$$u(k) = (1/\hat{b}_0(k))(C_2(z^{-1})y_m(k+d) - \hat{R}(z^{-1}, k)y(k) - \hat{B}s(z^{-1}, k)u(k-1) - \hat{d}c^*) \tag{14}$$

which also means that

$$C_2(z^{-1})y_m(k+d) = \hat{\mathbf{p}}^T(k)\boldsymbol{\phi}(k) \tag{15}$$

where $\hat{\mathbf{p}}^T = [\hat{b}_0, \hat{b}s_1, \hat{b}s_2, \ldots, \hat{b}s_{n_{Bs}}, \ldots, \hat{r}_0, \ldots, \hat{r}_{n_R}, \hat{d}c^*]$ is the estimate of the plant–controller parameters.

The plant–controller parameters of equation (14) are unknown and should be estimated first before $u(k)$ can be computed. The parameter adaptation algorithm for this is as follows:[3]

$$\begin{aligned} \hat{\mathbf{p}}(k) &= \hat{\mathbf{p}}(k-1) + \mathbf{F}(k)\boldsymbol{\phi}(k-d)e(k) \\ \hat{\mathbf{p}}(0) &= \mathbf{p}_0 \end{aligned} \tag{16}$$

$$\begin{aligned} \mathbf{F}(k+1) &= \frac{1}{\lambda_1(k)}\left(\mathbf{F}(k) - \frac{\mathbf{F}(k)\boldsymbol{\phi}(k-d)\boldsymbol{\phi}^T(k-d)\mathbf{F}(k)}{\lambda_1(k)/\lambda_2(k) + \boldsymbol{\phi}^T(k-d)\mathbf{F}(k)\boldsymbol{\phi}(k-d)}\right) \\ \mathbf{F}(0) &= \beta\mathbf{I}, \qquad 0 < \lambda_1(k) < 1, \qquad 0 < \lambda_2(k) < 2 \end{aligned} \tag{17}$$

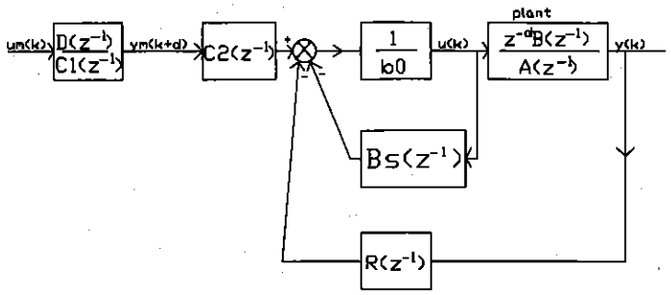

Figure 5. Linear-model-following control

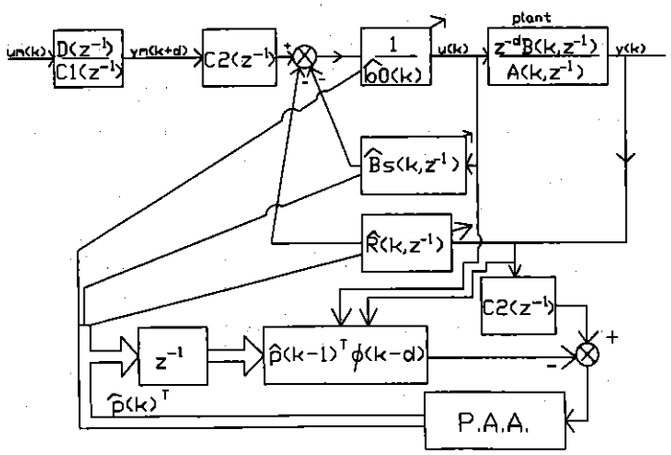

Figure 6. Model reference adaptive control

where $\mathbf{F}(k)$ is the adaptation gain matrix and $e(k)$ is the adaptation error given by

$$e(k) = \frac{C_2(z^{-1})y(k) - \hat{\mathbf{p}}^{\mathrm{T}}(k-1)\boldsymbol{\phi}(k-d)}{1 + \boldsymbol{\phi}^{\mathrm{T}}(k-d)\mathbf{F}(k)\boldsymbol{\phi}(k-d)} \tag{18}$$

A constant-trace algorithm, which provides an advantage of keeping the parameter adaptation action alive, is given by adjusting $\lambda_1(k)$ and $\lambda_2(k)$ such that

$$\text{trace}[F(k+1)] = \text{trace}[F(k)] \tag{19}$$

Figure 6 shows the block diagram for MRAC.

4. IMPLEMENTATION OF MRAC WITH CONSTANT DESATURATION OF FLYWHEEL ANGULAR VELOCITY

Full implementation of MRAC for azimuth control is complemented by the open-loop 'bang-off' control and desaturation control developed in Reference 2. A sampling time of $\frac{1}{3}$ s is used. Azimuth angle information in the experiment is derived from a strapdown inertial navigation unit called the attitude reference unit (ARU). An 80186-based computer with math processor is used for implementation of the controller.

Figure 7 shows the complete implementation of MRAC for the control of the azimuth angle of the balloon-borne stabilized platform.

There are two potential sources of problems in using MRAC for the azimuth-pointing system of the gondola in this project. First, the desired azimuth trajectory is generally a slow ramp. This fact, coupled with only 5·42 N m of maximum torque for a gondola with a moment

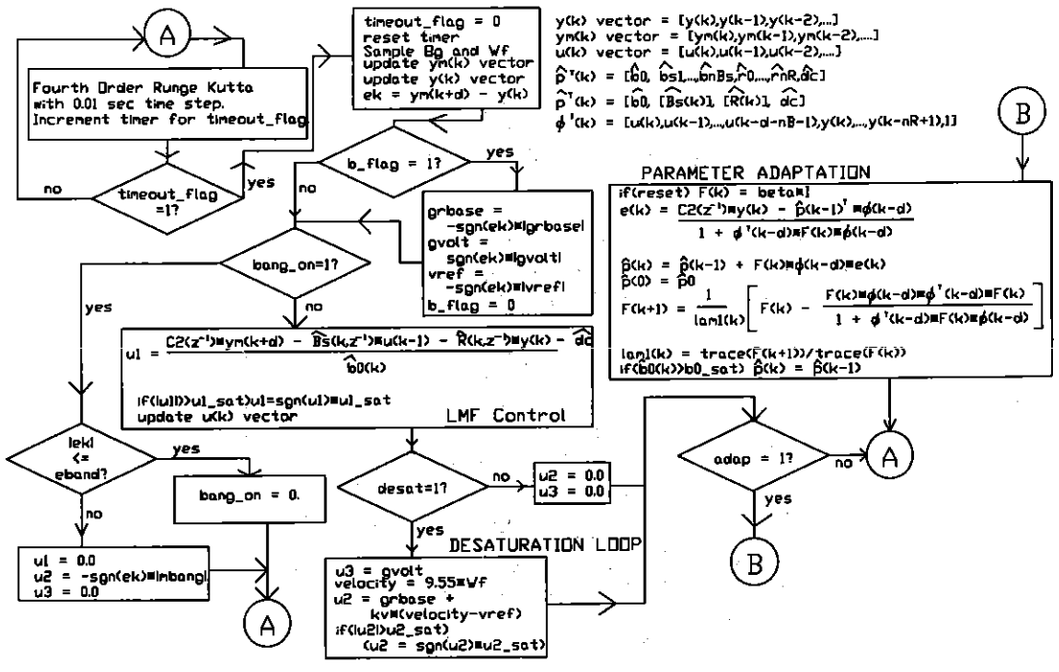

Figure 7. Implementation of MRAC with constant desaturation of flywheel angular velocity

of inertia of at least 195 kg m^2, can result in both insufficient frequency components and lack of energy of the generated control sequence $u(k)$. Secondly, some of the estimated parameters are expected to have small magnitude, which could be easily affected by fluctuations in estimates and even by truncations due to computation. The second problem is especially significant for the parameter $\hat{b}_0$ since it is the only denominator term in equation (14) and thus could seriously affect the computed control $u(k)$.

To minimize the effects of these two problems, the following steps are taken in the implementation of MRAC.

1. $\hat{b}_0$ is prevented from wandering too far from its estimated value. This is done by setting an upper limit on the value of $\hat{b}_0$ since it is known that $\hat{b}_0$ is negative. If the limit is exceeded, the parameters are not updated.
2. Saturation limit of the amplifier is reflected in generating the control sequence $u(k)$ to make sure that the magnitude of each element of the control vector used for parameter estimation is below or at most equal to the saturation value. This prevents incorrect estimation of the parameters.[4]
3. To simplify the process of trajectory generation, the desired trajectory $y_m(k+d)$ is generated directly instead of $u_m(k)$. This is reasonable since the azimuth trajectory of a celestial target is generally a slow lamp. During scanning, large scan steps are divided into smaller steps to avoid large transients.

5. PRELIMINARY OPEN-LOOP TEST OF CONSTANT-TRACE PARAMETER ADAPTATION

The azimuth-pointing system was first tested with the constant-trace parameter adaptation algorithm by driving the system with the pseudo-random binary signal (PRBS) sequence of $\{8, -8, -8, -8, 8, -8, -8, 8, 8, -8, 8, -8, 8, 8, 8\}$. This test was conducted to evaluate the order of the azimuth-pointing system and also to gauge the sensitivity of the adaptation process to the initial value of the gain matrix $\mathbf{F}(k)$, i.e. $\mathbf{F}(k) = \beta\mathbf{I}$.

To simulate steady state operation of the azimuth-pointing system, the gear motor was run with $g_{volt} = 2$ V and the RCUBE torque motor was run with $g_{rbase} = -1{\cdot}6$ V. However, there were no provisions made to minimize the magnitude of the constant disturbing torque due to

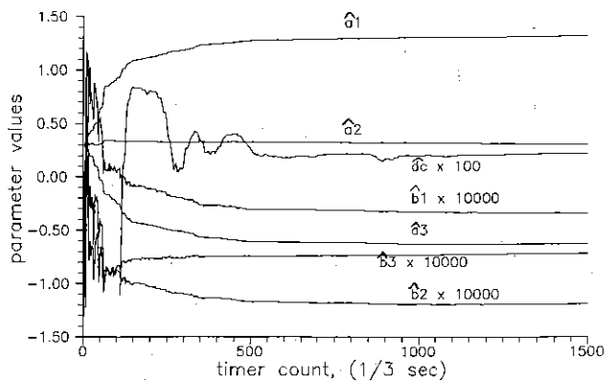

Figure 8. Parameter adaptation with $N_A = 3$, $N_B = 2$ and $\beta = 1000$

Coulomb friction with the use of the RCUBE's torque motor. Also, there were no provisions made to operate the flywheel at steady state velocity, since the PRBS signal has a mean of zero.

Open-loop test results suggest that $N_A = 3$, $N_B = 2$ seems to be the minimum order of the azimuth-pointing system. This result is consistent with the estimated order presented in the Appendix. Reducing the order n_A and n_B results in deteriorated parameter adaptation. The magnitude of β can also be safely placed at 1000 or less.

Figure 8 shows the results of the constant-trace parameter adaptation with $n_A = 3$, $n_B = 2$ and $\beta = 1000$. Except for the initial transients, all the parameters settled at their steady state values.

It is certainly possible to try higher orders for N_A and N_B. This, however, was not pursued in order to avoid having to work with even larger matrices for calculations of parameters.

6. RESULTS OF AZIMUTH POINTING WITH MRAC

This section present some of the representative results of azimuth pointing for MRAC with constant desaturation of the flywheel angular velocity. The following control parameters were used: $n_A = 3$, $n_B = 2$, $C_2(z^{-1}) = 1 - 1{\cdot}8z^{-1} + 1{\cdot}08z^{-2} - 0{\cdot}216z^{-3}$; $\mathbf{F}(0) = 100\mathbf{I}$, $k_v = 0{\cdot}03 \times 9{\cdot}55$, $|\,\text{mbang}\,| = 4$, $|\,g_{\text{volt}}\,| = 2$, $|\,g_{\text{rbase}}\,| = 1{\cdot}6$, $\omega_{\text{fref}} = 70$ rmp for actual data, $\omega_{\text{fref}} = 80$ rpm for simulation. In the case of simulation the parameter estimates were based on the computation presented in the Appendix. During the experiment, initial estimates of the parameters were based on adapted parameters obtained with earlier test runs of the experiment.

Figures 9 and a 10 show simulation results for MRAC. The controller in each case was able to achieve steady state pointing RMS of better than $0{\cdot}001^\circ$ for Figure 9 and $0{\cdot}005^\circ$ for Figure 10. The flywheel angular velocity was also operated well below saturation velocity.

For the following results the performance is quoted for each scan segment in terms of the azimuth-pointing error average and error RMS. In the figures, 'azi_gon' refers to the actual azimuth angle of the pointing system and 'az' refers to the computed azimuth angle of the tracked object. The reference scanning trajectory is not shown.

Figures 11(a) and 11(b) show ground test results for tracking with scanning. Azimuth pointing for each scan segment is better than $0{\cdot}03^\circ$. Flywheel velocity is also maintained below

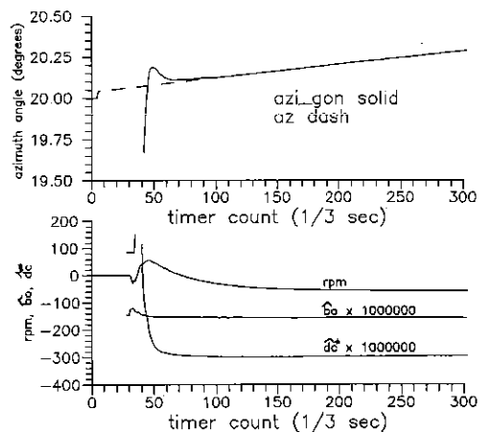

Figure 9. Simulation result, MRAC, azimuth tracking

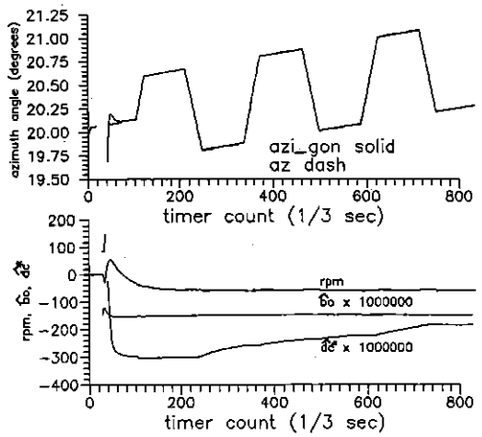

Figure 10. Simulation result, MRAC, azimuth tracking with scanning

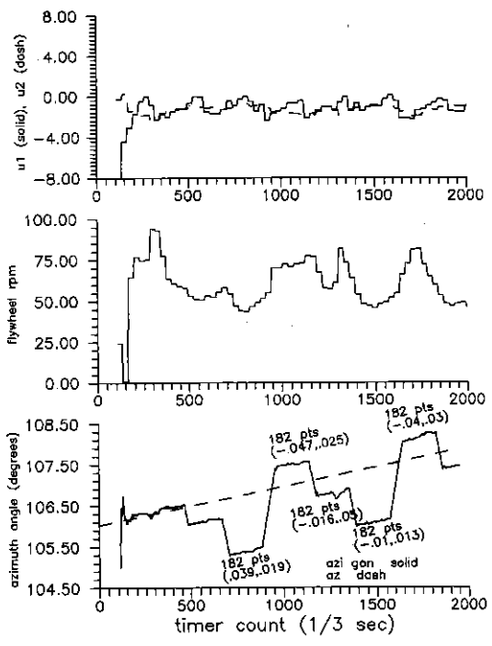

Figure 11(a). Ground test result, MRAC, azimuth tracking with scanning

saturation but large fluctuations are observed in the flywheel velocity. Fluctuation in the flywheel velocity can be explained by the fact that the ground test suffers from disturbances due to dragging electrical cables. These cables have been observed to cause the flywheel velocity to saturate if they are not positioned properly to create slacks. Figure 11(b) shows that although the $\hat{dc}^*$ estimate is changing slowly, the other parameters are not affected. Except for the reverse polarity, the disturbance estimate also has the same characteristic response as that of Figure 10 obtained with simulation. The control parameters settle nicely to their steady state values.

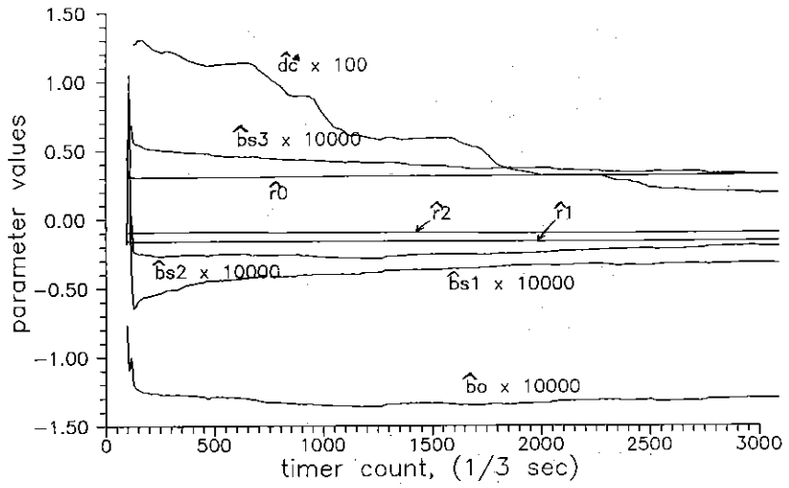

Figure 11(b). Ground test result, MRAC, parameter adaptation

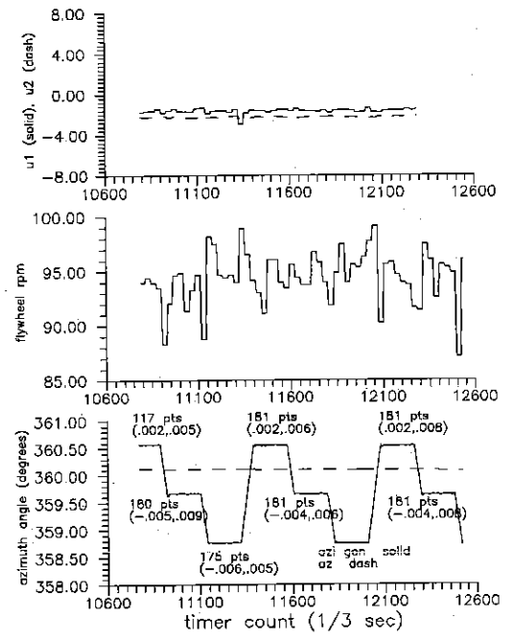

Figure 12. Flight result, MRAC, azimuth tracking with scanning

Figure 12 shows results for tracking with scanning during an actual flight. The relatively flat trajectory is due to the fact that the object being tracked is the north star Polaris. Azimuth-pointing RMS is better than $0{\cdot}01^\circ$ for the scan segment shown in the figure. Other results with MRAC show tracking better than $0{\cdot}02^\circ$. At float altitude, disturbances due to the electrical cables are no longer present, thus the flywheel angular velocity does not have large oscillations. Owing to some problems with the computer during the flight, adaptation parameters were not recorded.

7. CONCLUSIONS

Model reference adaptive control is developed and implemented for the control of the azimuth-pointing system of a balloon-borne stabilized platform. Results show the MRAC with constant desaturation of the flywheel angular velocity is successful in achieving the two objectives of the azimuth controller, i.e. the primary goal of achieving steady state pointing RMS of better than $0{\cdot}1^\circ$ and the secondary goal of maintaining the flywheel angular velocity below saturation to provide for continuous operation of the azimuth-pointing system. Azimuth-pointing RMS with MRAC for the first flight is better than $0{\cdot}02^\circ$.

MRAC performed as well as PID control implemented in (Reference 2). However, both controllers can still be optimized for better performance.

One important side result of the successful implementation of MRAC is the seemingly independent operation of the desaturation control scheme for the flywheel angular velocity. Although this control law was developed under a PID control structure in Reference 2, it was effectively used with MRAC. In fact, formulation of MRAC for a SISO system assumes that the desaturation control scheme will work. The effectiveness of this desaturation control scheme suggests that other control structures can be easily implemented by treating the azimuth-pointing system as a SISO system with constant or slowly varying disturbance, while the desaturation control scheme maintains the flywheel velocity for continuous operation of the azimuth-pointing system.

ACKNOWLEDGEMENTS

This research was supported by the National Aeronautics and Space Administration, the National Science Foundation, the California Space Institute, the U.S. Army, the Space Science Laboratory and the University of California. We gratefully acknowledge the encouragement and support of Donald Morris. This work would not have been possible without the direct support and assistance of Nancy Boggess and Buford Price. We especially thank the National Scientific Balloon Facility (NSBF) for launch support.

APPENDIX: ESTIMATING THE ORDER OF THE DISCRETE TIME SYSTEM

In this appendix the order of the discrete time azimuth-pointing system is estimated on the basis of the truncated system presented in Reference 2 and the assumptions made for the implementation of MRAC.

From Reference 2 the truncated system equation is

$$\mathrm{d}[X_2]/\mathrm{d}t = [A_{22}]\,[X_2] + [B_2]\,[U] \tag{20}$$

Here

$$[X_2]^{\mathrm{T}} = [\theta_{\mathrm{g}}, \omega_{\mathrm{g}}, \omega_{\mathrm{f}}] \tag{21}$$

$$[X_2]^{\mathrm{T}} = [u_1, u_2] \tag{22}$$

$$[A_{22}] = \begin{bmatrix} 0 & 1 & 0 \\ 0 & (-c_{\mathrm{g}} - k_{\mathrm{t}}B_{\mathrm{e}}/R_{\mathrm{a}})/J_{\mathrm{g}} & -2k_{\mathrm{t}}B_{\mathrm{e}}/R_{\mathrm{a}}J_{\mathrm{g}} \\ 0 & 0 & -2k_{\mathrm{t}}B_{\mathrm{e}}/R_{\mathrm{a}}J_{\mathrm{g}} \end{bmatrix} \tag{23}$$

$$[B_2] = \begin{bmatrix} 0 & 0 \\ -2k_{\mathrm{t}}k_{\mathrm{a}}/R_{\mathrm{a}}J_{\mathrm{g}} & -k_{\mathrm{t}}k_{\mathrm{a}}/R_{\mathrm{a}}J_{\mathrm{g}} \\ 2k_{\mathrm{t}}k_{\mathrm{a}}/R_{\mathrm{a}}J_{\mathrm{f}} & 0 \end{bmatrix} \tag{24}$$

where θ_{g} (rad) is the azimuth angle of the gondola/telescope system, ω_{g} (rad s^{-1}) is the angular velocity

of the gondola/telescope system, ω_f (rad s^{-1}) is the flywheel angular velocity, u_1 (V) is the D/A command to the flywheel motor/amplifier, u_2 (V) is the D/A command to the RCUBE motor/amplifier, J_g is the gondola moment of inertia, 195 kg m^2 (estimate), J_f is the flywheel moment of inertia, 0·942 kg m^2, k_a is the torque motor PWM amplifier gain, 2·6 V/V, k_t is the motor torque constant, 0·57 N m A^{-1}, B_e is the back EMF gain, 0·57 V rad^{-1} s, R_a is the armature resistance, 5·7 Ω, and c_g is the gondola damping in air, ~0·0 N m rad^{-1} s.

For the implementation of MRAC it is assumed that at steady state the RCUBE torque motor control u_2 is implemented with

$$u_2 = g_{\text{rbase}} + k_v(\omega_f - \omega_{\text{fref}}) \tag{25}$$

where ω_{fref} (rad s^{-1}) is the reference flywheel velocity.

Using the default values of the different system parameters in equation (20), the discrete time equivalent of the truncated system with $\frac{1}{3}$ s sampling time can be numerically computed. The result is

$$\begin{bmatrix}\theta_g(k+1)\\ \omega_g(k+1)\\ \omega_f(k+1)\end{bmatrix} = \begin{bmatrix}1 & 0{\cdot}333284 & 0{\cdot}000032\\ 0 & 0{\cdot}999903 & 0{\cdot}000191\\ 0 & 0 & 0{\cdot}960539\end{bmatrix}\begin{bmatrix}\theta_g(k)\\ \omega_g(k)\\ \omega_f(k)\end{bmatrix} + \begin{bmatrix}-0{\cdot}000146 & -0{\cdot}000074\\ -0{\cdot}000869 & -0{\cdot}000443\\ 0{\cdot}179923 & 0\end{bmatrix}\begin{bmatrix}u_1(k)\\ u_2(k)\end{bmatrix} \tag{26}$$

Substituting $u_2(k) = k_v\omega_f(k)$ in equation (26), the discrete time transfer function from $u_1(k)$ to $\theta_g(k)$ is computed as

$$\Theta_g(z^{-1}) \simeq \frac{z^{-1}(-0{\cdot}000146 - 0{\cdot}00000146z^{-1} + 0{\cdot}00013987z^{-2})}{(1-z^{-1})(1-0{\cdot}965346z^{-1})(1-0{\cdot}9999036z^{-1})}\, U_1(z^{-1}) \tag{27}$$

where $\Theta_g(z^{-1})$ is the z-transform of $\theta_g(k)$ and $U_1(z^{-1})$ is the z-transform of $u_1(k)$.

Adding one step delay due to computer loop computation, equation (27) becomes

$$\Theta_g(z^{-1}) - \frac{z^{-2}(-0{\cdot}000146 - 0{\cdot}00000146z^{-1} + 0{\cdot}00013987z^{-2})}{(1-z^{-1})(1-0{\cdot}965364z^{-1})(1-0{\cdot}9999036z^{-1})}\, U_1(z^{-1}) \tag{28}$$

If the discrete plant is known completely, the Bezout identity

$$C_2(z^{-1}) = A(z^{-1})S(z^{-1}) + z^{-d}R(z^{-1}) \tag{29}$$

can be solved to find the gains of the deterministic controller.

Using $C_2(z^{-1}) = (1 - 0{\cdot}6z^{-1})^3$, the results become

$$R(z^{-1}) = 1{\cdot}5945 - 2{\cdot}645z^{-1} + 1{\cdot}115z^{-2} \tag{30}$$

$$S(z^{-1}) = 1 + 1{\cdot}1604z^{-1} \tag{31}$$

REFERENCES

1. Pelling, M. and F. Duttweiler, Physics Department, University California, San Diego, CA, Private communications, 1985.
2. Chingcuanco, A. O., P. M. Lubin, P. R. Meinhold and M. Tomizuka, 'Modelling and control of a balloon borne stabilized platform', *ASME J. Dyn. Syst., Meas. Control*, **112**, (1990).
3. Landau, I. D. and R. Lozano, 'Unification of discrete time explicit model reference adaptive control designs', *Automatica*, **17**, 593–611 (1981).
4. Wittenmark, B. and K. J. Åström, 'Practical issues in the implementation of self-tuning control', *Automatica*, **20**, 595–605 (1984).